Carbohydrate Polymers 80 (2010) 699–710

Contents lists available at ScienceDirect

Carbohydrate Polymers

journal homepage: www.elsevier.com/locate/carbpol

Enzyme resistance and structural organization in extruded high amylose maize starch

Ashok K. Shrestha [a,b], Chin S. Ng [a], Amparo Lopez-Rubio [c,1], Jaroslav Blazek [c], Elliot P. Gilbert [c], Michael J. Gidley [a,*]

[a] Centre for Nutrition and Food Sciences, University of Queensland, St. Lucia, Qld 4072, Australia
[b] Commonwealth Scientific and Industrial Research Organisation, Food Futures National Research Flagship, Riverside Corporate Park, North Ryde, NSW, Australia
[c] Bragg Institute, Australian Nuclear Science and Technology Organisation, PMB 1, Menai, NSW 2234, Australia

ARTICLE INFO

Article history:
Received 10 August 2009
Received in revised form 24 November 2009
Accepted 3 December 2009
Available online 28 December 2009

Keywords:
Starch
High amylose maize
Enzyme digestion
Extrusion
X-ray diffraction

ABSTRACT

Gelose 80, a high amylose maize starch, was extruded in a twin screw extruder at different feed moistures, cooled, stored for 12 days at 4 °C, and cryo-milled. The raw and extruded starches were analysed for *in vitro* enzyme-resistant starch content (ERS), morphology, *in vitro* digestibility, long range (X-ray diffraction) and short range (FTIR) molecular order. Extrusion markedly increased the rate of starch digestion and reduced the ERS content, irrespective of whether B-type or B- and V-type polymorphs were present. Increasing feed moisture and storage resulted in only slight increases in ERS content, with X-ray diffraction and FTIR also showing small changes in long and short range molecular order, respectively. Analysis of residues from *in vitro* digestion showed the mechanism of enzyme resistance of granular and extruded high amylose starch to be markedly different, both qualitatively and quantitatively. Enzyme digestion of granular high amylose maize starch showed initial disorganization in structure followed by slow reorganization at later stages of digestion. In contrast, molecular reorganization took place throughout the enzyme digestion of extruded high amylose maize starch. Higher levels of crystallinity were found in digested extrudates compared with digested granules, showing that there is no direct correlation between starch crystallinity and enzyme digestion rates.

1. Introduction

Based on their susceptibility to enzymic digestion, starch is classified as rapidly digestible starch (RDS), slowly digestible starch (SDS) or resistant starch (RS) (Englyst, Kingman, & Cummings, 1992). Resistant starch has been defined as "the sum of starch and products of starch degradation not absorbed in the small intestine of healthy individuals" (Asp, 1992). Major types of RS include native starch granules from a number of sources (including high amylose maize) known as RS2, and gelatinised and retrograded starches, known as RS3. Foods with significant RS levels are reported to have beneficial effects on colonic health (Topping & Clifton, 2001) and may also have a reduced glycemic load with possible protective effects against type II diabetes, obesity and heart diseases (Kendall, Emam, Augustin, & Jenkins, 2004). RS is most commonly measured by *in vitro* methods that simulate *in vivo* conditions of starch digestion (physiologically resistant starch, PRS) and referred to as 'enzyme-resistant starch' (ERS) (Chanvrier et al., 2007).

Many food processing methods partially or wholly destroy the structural integrity of native starch granules (RS2) and generate retrograded or recrystallized starch (RS3). Native starch granules are protected from enzyme digestion by several factors such as restricted mobility of chains preventing enzyme binding, dense packing of polymers within granules acting as a barrier to enzymes, and helical conformations of amylose molecules and long amylopectin branches (Bird, Lopez-Rubio, Shrestha, & Gidley, 2009; Oates, 1997). Native starch granules from e.g., potato, banana, and high amylose maize are highly resistant to digestion (Champ, 2004; Englyst et al., 1992). In contrast, only high amylose maize starch (HAMS) tends to retain significant amounts of RS after processing, which makes it an ingredient of choice for foods with high RS levels (Garcia-Alonso & Goni, 2000; Gonzalez-Soto, Escobedo, Hernandez-Sanchez, Sanchez-Rivera, & Bello-Perez, 2006; Htoon et al., 2009).

Food processing techniques generally alter textural attributes for palatability, but also transform starch fractions into more digestible forms. In order to understand the digestibility of processed starch, it is important to characterise the changes in structure and physico-chemical properties that occur as a result of processing. Starch granules consist of a hierarchical structure, in

* Corresponding author. Tel.: +61 7 3365 2145: fax: +61 7 3365 1177.
E-mail address: m.gidley@uq.edu.au (M.J. Gidley).
[1] Present address: Novel Materials and Nanotechnology Lab., Apdo. Correos 73, 46100 Burjassot, Spain.

0144-8617/$ - see front matter © 2009 Elsevier Ltd. All rights reserved.
doi:10.1016/j.carbpol.2009.12.001

which amylose and amylopectin molecules are present within complex molecular arrangements that display structural periodicity of alternating crystalline and amorphous lamellae with a characteristic repeat distance of ca. 10 nm (Jenkins & Donald, 1996). At larger length scales, lamellar structures are hypothesized to form blocklets or super-helices that are arranged into longer range alternating amorphous and semi-crystalline radial growth rings of 120–400 nm thickness emanating from the hilum. The changes brought about by processing in starch are complex, as the changes can occur at different levels of starch structure ultimately affecting its resistance to amylase digestion. A number of factors are known to affect the enzyme resistance of starches such as amylose content (Berry, 1986; Chanvrier et al., 2007; Sievert & Pomeranz, 1989), moisture (Kim, Tanhehco, & Ng, 2006; Sievert & Pomeranz, 1989), heating time and temperature (Eerlingen, Crombez, & Delcour, 1993; Szczodrak & Pomeranz, 1991), storage time and temperature (Ferrero, Martino, & Zaritzky, 1993; Kim et al., 2006), high pressure cooking/extrusion (Bello-Perez, Ottenhof, Agama-Acevedo, & Farhat, 2005; Kim et al., 2006), pH/acidity (Onyango, Bley, Jacob, Henle, & Rohm, 2006; Vasanthan & Bhatty, 1998), and the presence of additives such as sugar, lipid, and dietary fiber (Eerlingen, Bjorck, Delcour, Slade, & Levine, 1994; Eerlingen, Cillen, & Delcour, 1994; Escarpa, Gonzalez, Morales, & Saura-Calixto, 1997). Considering the potential significance of HAMS in formulating high RS foods, it is important to increase understanding of the effects that processing has on enzyme resistance and structural transformations. Few studies have explored the influence of processing on the formation of RS from HAMS. Treatment of HAMS in a capillary rheometer was found to reduce ERS content significantly along with molecular order (Chanvrier et al., 2007; Htoon et al., 2009). It was shown that significant levels of ERS (>10%) can be obtained for processed HAMS with a low level of molecular and crystalline order and that the mechanism of enzyme resistance of granular and processed HAMS was qualitatively different (Htoon et al., 2009). Entrapment of amorphous regions within imperfect crystals and the presence of double helical structures not necessarily part of crystallites have been suggested as mechanisms of enzymatic resistance for non-crystalline fractions (Lopez-Rubio, Flanagan, Shrestha, Gidley, & Gilbert, 2008).

Extrusion cooking is a common processing method for starch-based foods such as pasta, breakfast cereals, etc. In this study a twin screw extruder with varying feed moisture was used to process HAMS and study the development of crystallinity and enzyme resistance in the processed starch. There are no reported studies on the effect of extrusion of high amylose starch, other than laboratory models (Blaszczak, Fornal, Valverde, & Garrido, 2005; Chanvrier et al., 2007; Htoon et al., 2009). Considering the gap of knowledge in this area, the objectives of this work were to study: (1) enzyme resistance and structural changes in high amylose starches extruded at various moisture contents and (2) the progression of molecular order in raw- and extrusion-processed starch during *in vitro* digestion. The results highlight the opportunity to create extruded HAMS products with nutritionally useful levels of enzyme-resistant starch, and clarify the different molecular and microstructural mechanisms underlying enzyme resistance in granular and extruded HAMS.

2. Materials and methods

2.1. Materials

High amylose maize starch, Gelose 80, was purchased from Penford Australia Ltd., Lane Cove, Sydney, Australia. The raw starch was analysed for moisture content by vacuum drying at 70 °C before extrusion experiments, and kept in a sealed container at room temperature. The following enzymes and chemicals were obtained from local distributors: α-amylase (porcine pancreas), pepsin, pancreatin (porcine pancreas), amyloglucosidase (*Aspergillus niger*), α-cellulose, and regular maize starch from Sigma, α-amylase (*Bacillus licheniformis*) and amyloglucosidase from Megazyme, and enzyme glucose reagent from Thermoelectron.

2.2. Extrusion of starches

Extrusion was carried out in a Prism Eurolab™ co-rotating twin screw extruder (Thermo Prism, Staffordshire, UK). The screw diameter was 16 mm and the extruder barrel was 640 mm long, giving a length to diameter (L/D) ratio of 40:1. The extruder was divided into 10 different zones, the first of which was a dry feed zone and the rest were electrically heated barrel zones and a die block (with two openings of 2 mm diameter). The barrel temperature profile was set at 50, 75, 100, 120, 120, 110, 105, 100, 95, and 80 °C (die block). The screw speed was set at 180 rpm. The die block pressure and the motor torque were in the range of 6–24 bar and 11–42%, respectively, depending on the solid and water feed rate, type of starch and relative humidity of the extruder room. Starch was fed through a single screw feeder (KX16 Powder Feeder, Brabender Technology, Duisburg, Germany). Water was injected through a port 150 mm from the start of the barrel using a peristaltic pump (L/S 7523) with Tygon Lab tubing. The dry feed rate (Auger speed) was set at 25, giving a rate of 9–10 g/min. The water feed rate was set at different rates, 1.5–7 g/min, depending on the amount of water to be added. Motor torque, screw speed, powder feed rate, barrel temperatures and melt pressure were monitored with Prismdde software (Sysmac-SCS version 2.2, Omron Corporation, UK). The expansion ratio was calculated as diameter of the extrudate divided by the diameter of the die (2 mm). In this study, all other extrusion parameters e.g., screw speed, temperature profile and feed rate were kept the same except for the liquid feed rate which was used to vary the final moisture content.

2.3. Sample collection and storage

The extruder was run at the required set of barrel temperatures, screw speed, Auger speed and high liquid feed rate for about 15 min. Once the system was stable, the liquid feed rate was set at the level needed to achieve moisture contents of 30%, 40%, or 50% within the extruder. The extrusion was carried out for 15–20 min before samples were collected. The moisture content of extrudates was immediately measured by an infrared moisture meter (Sartorius Moisture Analyzer, NY). The moisture meter was previously calibrated for flour samples analysed by drying in a vacuum oven (Thermoline Australia) overnight at 70 °C. The measured extrudate moisture contents for barrel mixtures containing 30%, 40%, and 60% water were reduced to 20.8%, 30.4%, and 36.3%, respectively, due to evaporation at the die plate. Extrudates were cut into approximately 12 cm lengths, cooled to room temperature, packed in Cryovac® bags, and stored for 0 (fresh) or 12 days (stored) at 4 °C. The extrudates were then freeze dried and cryo-milled for 10 min into fine powders using liquid nitrogen in a cryogrinder (Freezer/Mill, Metuchen, NJ, USA). Another set of extrudates were dried overnight at 50 °C in a vacuum oven and ground into powder by a hammer mill (Glen Creston Ltd., Stanmore, UK). The milled extrudate was sieved and particles (sizes 180–600 μm) were transferred into small plastic containers, tightly capped, and stored at room temperature until further use.

2.4. In vitro resistant starch analysis

The enzyme-resistant starch (ERS) content of raw and extruded Gelose 80 samples was determined using an assay system involv-

ing a series of incubations, at physiological pH and temperature, which essentially mimic the buccal, gastric and pancreatic phases of starch digestion in humans (Bird, Usher, Topping & Morrell, unpublished results). Briefly, about 500 mg of accurately weighed sample was placed in a flask and mixed with artificial saliva [250 U/mL of α-amylase at pH 7.0]. After 15–20 s, the mixture was incubated with acidified (0.02 M HCl) pepsin (1 mg/mL) at 37 °C for 30 min. The solution was adjusted to pH 6.0 and the sample treated with pancreatin (2 mg/mL) and amyloglucosidase (28 U/mL) for 16 h at 37 °C in 0.2 M acetate buffer (pH 6.0) in a shaking water bath. The amount of starch remaining in the digesta at the end of the incubation period was determined using conventional enzymatic and spectrophotometric methodologies. The resistant starch content of the sample was expressed as a percentage of sample weight and total starch content.

2.5. In vitro starch digestibility

Approximately 500 mg of starch, in duplicate, was first digested with artificial saliva, pepsin, neutralized with alkali, buffered and incubated with 5 mL of pancreatin and amyloglucosidase (as in the ERS analysis method). The mixture was then incubated for 0, 0.5, 1.5, 4.0, 8.0 and 24 h. After completion of each incubation time, the flask containing hydrolysed starch was chilled in an ice-water bath, and the content carefully transferred to 50 mL polypropylene centrifuge tubes and centrifuged at 2000*g* for 10 min. The glucose content of the supernatant was measured using enzymatic glucose reagent. The residues in the centrifuge tube were frozen, freeze dried and %yield was calculated by dividing weight of freeze dried residue by weight of samples. A digestogram was plotted with time as abscissa and %glucose released as ordinate.

2.6. Particle size distribution

The particle size distribution of raw and milled starches was measured using a Malvern Laser Diffraction Particle Size Analyzer with a 100 mm lens, (Malvern Mastersizer B, Malvern Instruments Co., Worcestshire, UK). Isopropanol was used as a dispersing medium for all powders. Mechanical stirring was applied to ensure even dispersion and particle distribution. The measurements were done in triplicate. The median volume-based diameter was used to represent the average particle size.

2.7. X-ray diffraction (XRD)

XRD measurements of samples were made with a X'Pert PRO X-ray diffractometer (PANalytical, Almelo, Netherlands). The instrument was equipped with a copper X-ray generator (λ = 1.54443 Å), programmable incident beam divergence slit and diffracted beam scatter slit, and an X'celerator high speed detector. X-ray diffractograms were acquired at 20 °C over the 2θ range of 5–40° with a step size of 0.0330° 2θ and a count time of 1 s per step.

The Igor software package (Wavemetrics, Lake Oswego, OR) was used for curve fitting as described by Lopez-Rubio, Flanagan, Gilbert, and Gidley (2008). The obtained values from the fitting coefficients are those that minimize the value of chi-squared, which is defined as:

$$\sum \left(\frac{y - y_i}{\sigma_i} \right)$$

where y is a fitted value for a given point, y_i is the measured data value for the point, and σ_i is an estimate of the standard deviation for y_i. The curve fitting operation is carried out iteratively. For each iteration, the fitting coefficients are refined to minimize chi-squared.

The Levenberg–Marquardt algorithm is used to search for the coefficient values that minimize chi-squared. This is a form of non-linear, least squares fitting. The iterative fit terminates when the fractional decrease of chi-squared between successive iterations is less than 0.001. Crystallinity was calculated as the percentage proportion of the area under the crystalline peaks to the total area, which was calculated as the area between the experimental data and the baseline.

2.8. Fourier transform infrared spectroscopy (FTIR)

FTIR spectra were obtained using a Spectrum FTIR 100 series Perkin-Elmer spectrometer (UK) fitted with a DTGS (deuterated triglycine sulphate) detector using the Universal Attenuated Total Reflectance (ATR) single reflectance cell with a diamond crystal. An aliquot of sample was placed over the diamond crystal and smoothed with a spatula. It was then pressed gently with a small steel cylinder until an optimum force of 100 (an arbitrary instrument scale) was reached and scanned over the range of 1200–800 cm^{-1}. A background spectrum was recorded in air (without sample) and subtracted from the sample spectra. For each spectrum, 32 scans were recorded. Scanning was done at room temperature (about 22 °C) at a resolution of 4 cm^{-1}, co-added and Fourier transformed. All the scanned spectra were baseline-corrected using the in-built program in the Spectrum FTIR 100 system. The amplitudes of absorbance for each spectrum at 995 and 1022 cm^{-1} were noted from each sample. The intensity ratio of 995/1022 cm^{-1} was used as a convenient index of FTIR data as a measure of short range starch conformation (Lopez-Rubio, Flanagan, Shrestha et al., 2008).

2.9. Microscopy

The morphology of raw, processed and digested starch was studied using polarized light and scanning electron microscopy (SEM). For light microscopy, starch powder was thinly spread onto a microscope glass slide and dispersed in excess water. The dispersed starch was gently covered with a glass slide and viewed with an optical microscope fitted with a polarizer (Olympus Optical Co., Ltd., Tokyo, Japan). A Sensys digital camera (Photometric Ltd., Tucson, AZ, USA) was used for image capture.

For SEM, the dried starch powder was thinly spread onto circular metal stubs coated with double-sided adhesive carbon. The stubs were transferred to a desiccator containing P_2O_5, vacuumed and left overnight at room temperature. The powder on the stubs was platinum coated in an Eiko IB-5 Sputter Coater (at 6 mA, 5 min for medium coating) in an argon gas environment, yielding approximately 15 nm coating thickness. The coated samples were imaged in a JEOL 6400 JSM scanning electron microscope (JEOL Ltd., Tokyo, Japan). The accelerating voltage used was 10 kV and the working distance was set at 15 mm. Representative micrographs were taken at low magnification followed by higher magnification up to 20,000.

3. Results and discussion

3.1. Effect of extrusion on ERS content

The enzyme-resistant starch (ERS) content of raw Gelose 80 was 52.1% (dry basis), comparable to a previous report of 45.7% (Htoon et al., 2009). Gelose 80 is an unmodified high amylose corn starch that has an amylose content of 74.8% (Htoon et al., 2009). The role of amylose in starch granules is not well understood. Amylose is thought to cause defects in the crystalline lamellar regions formed by amylopectin double helices. In this sense, cultivars with normal

amylose content often show lower crystallinity compared to their waxy counterparts. On the other hand, amylose may partly co-crystallize with amylopectin in such high amylose starches. Additionally, amylose may serve as a reinforcing and stabilizing structural feature in the amorphous growth rings, making them more rigid and crowded, and less able to absorb water and swell. Intuitively, one would think that the crystal disruption caused by amylose may lead to a greater susceptibility to amylase digestion but it is well reported that high amylose starch granules are more resistant to amylase attack than amylopectin-rich starch granules (Evans & Thompson, 2004; Jiang & Liu, 2002; Themeier, Hollman, Neese, & Lindhauer, 2005).

The ERS content of cryo-milled extruded Gelose 80, fresh and after 12 days storage is given in Table 1. This shows that extrusion cooking of Gelose 80 caused a significant drop in the ERS content for all samples. In comparison to raw starch, the percentage decrease in ERS content ranged from 69% to 75%. It is well known that certain native starch granules (RS 2) are more enzyme resistant than gelatinized starches, with explanations being put forward based on restricted mobility of the chain or the individual glucose units being locked into a specific configuration (Oates, 1997; Ring, Gee, Whittam, Orford, & Johnson, 1988). In addition, the dense packing of polymers within granules is likely to provide some barrier to access of hydrolytic enzymes. The dense packing of polymers is considered to be linked to the crystal organization within starch granules (RS2); this highly organized granular structure, based primarily on amylopectin crystallites, is expected to be disrupted by the high temperature (up to 120 °C) and pressure ($\geqslant$10 bar) generated during heating in the presence of water and shearing force during extrusion processing. Once the granular structure is disrupted, it is then possible for amylose molecules to rearrange (retrograde) into more thermally stable forms. However, the maximum extrusion temperature used was 120 °C, which is lower than the melting temperature of retrograded amylose of ~155 °C (enthalpy 12–27.4 J/g) which is known to be enzyme resistant (Gidley et al., 1995; Sievert & Pomeranz, 1990). Thus, the extrusion conditions may promote annealing of ordered structures (alongside conventional gelatinisation) contributing towards considerable resistance to amylase hydrolysis (~15% ERS in extrudates). In addition, it is possible that partially hydrolysed starch polymers may have been incorporated into a dense/crystalline structure contributing towards enzyme resistance (Cairns, Botham, Morris, & Ring, 1996; Eerlingen et al., 1993; Gidley et al., 1995; Jane & Robyt, 1984).

In this study, some of the extrudates were hammer milled and subsequently analysed for ERS content. Due to heat generated by hammer milling, we chose to complete the process in several cycles. The resulting particle size range was large and only particles between 150 and 850 μm were selected for ERS analysis (by sieving). In comparison, cryo-milled particles were finer and more homogenous in size. Particle size analysis showed that the average size of hammer milled and cryo-milled starch was 235 and 38.5 μm [surface mean diameter, $D(3,2)$], respectively. A comparison of ERS content showed cryo-milled starch to have a lower ERS than hammer milled starch (Table 1). Food particle size is known to affect the enzyme digestibility of starch as smaller particles have larger surface areas relative to volume (Al-Rabadi, Gilbert, & Gidley, 2009; Annison & Topping, 1994). Therefore, the smaller particles were digested more rapidly compared to the larger particles resulting in lower ERS values. Digestibility of bread was reported to be lowered by using whole kernels of wheat, rye, barley and oats instead of flours (Liljeberg, Akerberg, & Bjorck, 1996). Processed starches with large particle sizes may find food applications where particulate components provide part of the sensory experience. The relatively indigestible processed high amylose starches have potential to be used as an ingredient for different processed foods with low enzyme digestibility for control of glucose uptake and the delivery of physiologically resistant starch.

Table 1
Enzyme resistant starch (ERS) content of extruded Gelose 80[a,b].

Moisture (%)	Sample	ERS (%)	
		Cryo-milled	Hammer-milled
20.8 ± 0.4	Fresh	13.1 ± 1.0	16.3 ± 0.1
	Stored	14.5 ± 1.5	16.5 ± 0.5
30.4 ± 0.2	Fresh	14.7 ± 1.1	17.6 ± 0.0
	Stored	15.5 ± 2.5	18.5 ± 0.0
36.3 ± 0.0	Fresh	15.6 ± 0.6	22.6 ± 0.3
	Stored	16.1 ± 0.6	22.6 ± 1.0

[a] All data are expressed as moisture free basis.
[b] Mean ± starndard deviation (of duplicates).

3.2. Effect of feed moisture and storage on ERS content

Extrusion of starch was carried out at water feed rates nominally set to achieve 30%, 40% and 60% moisture in the extrudates but only 20.8%, 30.4% and 36.3% moisture was achieved in the freshly extruded samples, respectively. The most likely causes for low moisture in extrudates are the loss of water due to sudden expansion and pressure drop when extrudates exit from the die. The expansion ratio was 1.04, 1.11 and 1.00 for extrudates containing 20.8%, 30.4% and 36.3% final moisture, respectively, showing little variation and no obvious correlation with moisture content. Thus extrusion of Gelose 80 in the presence of these amounts of water causes only minor radial expansion. Increasing water flow rates seemed to have very little effect on expansion ratio. Table 1 shows that increasing moisture content from 20.8% to 30.4% (fresh) led to small increases in ERS for both fresh and stored extrudates i.e. not correlated with expansion ratios. Increasing moisture content under high temperature shearing facilitates gelatinization of starch. These gelatinized starches are more likely to retrograde and contribute towards the enzyme resistance of the starch. However, unlike normal starches, high amylose starches are known to be difficult to hydrate and have higher gelatinization temperature (Jiang & Liu, 2002). The specific mechanical energy (SME) value of Gelose 80 extrudates at 36.3%, 30.4% and 20.8% final moisture was 195, 232 and 315 kJ/kg, respectively. This data shows that more work is needed to melt starches at low moisture than at higher moisture level. The literature on extrusion cooking of high amylose starch is limited, particularly with respect to variation in moisture contents. Thuwall, Boldizar, and Rigdahl (2006) reported that extrusion of high amylose potato starch (86% amylose) is problematic and that increasing moisture content can reduce this difficulty. They suggested that the processing window for high amylose starches is quite narrow, and depended to a great extent on the moisture content which determines the viscosity of the material. The native granules have a dense packing of amylose and amylopectin contributing to the enzyme resistance of granules (RS2) which is mostly lost during extrusion and not recovered even under high moisture conditions which would in principle favour retrogradation. In contrast, for low amylose starches the ERS content tends to increase after extrusion (Bello-Perez, 2005; Agustiniano-Osornio et al., 2005; Gonzalez-Soto et al., 2006; Unlu & Faller, 1998; Vasanthan, Gaosong, Yeung, & Li, 2002). Kim et al. (2006) extruded pastry wheat flour at 20%, 40% and 60% feed moisture and screw speeds and barrel temperatures similar to the current study. They reported a relative increase of 136% RS when feed moisture increased from 20% to 40% but about a 500% relative increase from 20% to 60% moisture. However, these comparisons are somewhat misleading because the absolute levels of ERS are higher in ex-

truded HAMS (13–23% – Table 1) compared with extruded wheat flour (0.5–4.1%). What these comparisons do highlight is that there is no universal relationship between raw and processed starches in terms of relative enzyme digestibility.

The storage of extruded starches containing varying moisture contents at 4 °C for 12 days caused a slight increase in ERS content (Table 1). This result was close to the findings reported by Chanvrier et al. (2007) where extruded Gelose 80 (using a capillary rheometer at 140 °C and 28% moisture) stored at 4 °C for 72 h resulted in a small (15%) increase in ERS content (from 7.8 in control to 8.8%). However, storage at higher temperatures of 30 °C and 60 °C resulted in 26% and 37% relative increase in ERS content, respectively (Chanvrier et al., 2007). This shows that formation of ERS in processed high amylose starches can be a function of storage temperature. Cairns, Sun, Morris, and Ring (1995) suggested that storage of amylose gels leads to increase in RS content due to slow formation of more perfect crystals containing fewer defects (annealing).

3.3. Effect of extrusion on digestibility of Gelose 80

The enzymic hydrolysis of raw and extruded Gelose 80 at 37 °C for 0.0, 0.5, 1.5, 4.0, 8.0 and 24.0 h was measured by the amount of glucose released into the supernatant. A general pattern of a gradual increase in glucose release was obtained with the progression of starch hydrolysis. Digestion kinetic curves include two apparent underlying stages of starch digestion with differing digestion rates (often distinguished as rapidly and slowly digested starch). In reality, the progression of glucose release is more likely due to first order kinetics (Al-Rabadi et al., 2009; Goni, Garcia-Diz, Manas, & Saura-Calixto, 1996) leading to an exponential decrease in starch content. The rate of starch hydrolysis was much slower in raw Gelose 80 compared to extruded starches. The hydrolysis extent of raw Gelose 80 after 24 h was 28.9%, compared to previously reported values for HAMS of 17% at 24 h hydrolysis for Hylon VII (75.5% amylose) (Jiang & Liu, 2002), 25% at 8 h hydrolysis for AL-80 (83% amylose) (Morita, Ito, Brown, Ando, & Kiriyama, 2007) and ~45% at 24 h hydrolysis for an unknown high amylose starch (Planchot, Colonna, Gallant, & Bouchet, 1995). Planchot et al. (1995) further reported that the initial stage of hydrolysis is longer (25 h) after which the rate of hydrolysis decreases progressively and becomes negligible. These reported values for the extent of hydrolysis are slightly different from our findings but the comparison of starch digestibility values between studies, even for the same starch, is difficult as the methodology used, type and dosage of starch hydrolysing enzymes employed markedly affects the final result (Goni et al., 1996; Planchot et al., 1995). However, the current and previous studies all show the high resistance to digestion, linked to large ERS content, of raw HAMS granules.

Compared to raw Gelose 80, extruded starches had a relatively rapid initial hydrolysis, particularly up to 4 h, followed by subsequent slower digestion (Fig. 1). The increase in susceptibility of the extruded high amylose starches was in accordance with their behaviour in ERS measurement (Table 1). The hydrolysis extent after 24 h digestion for extruded starches (fresh) with moisture content of 20.8%, 30.4% and 36.3% moisture were 70.5%, 66.7% and 61.7%, respectively, which are more than twice that of raw Gelose 80. Fig. 1 also shows the effect of feed moisture on digestibility of the extruded starches for fresh as well as stored samples. For fresh samples, the rates of hydrolysis for extrudates containing 20.8% and 36.3% moisture were similar up to 8 h digestion and slightly lower for extrudate with 30.4% moisture. However, hydro-

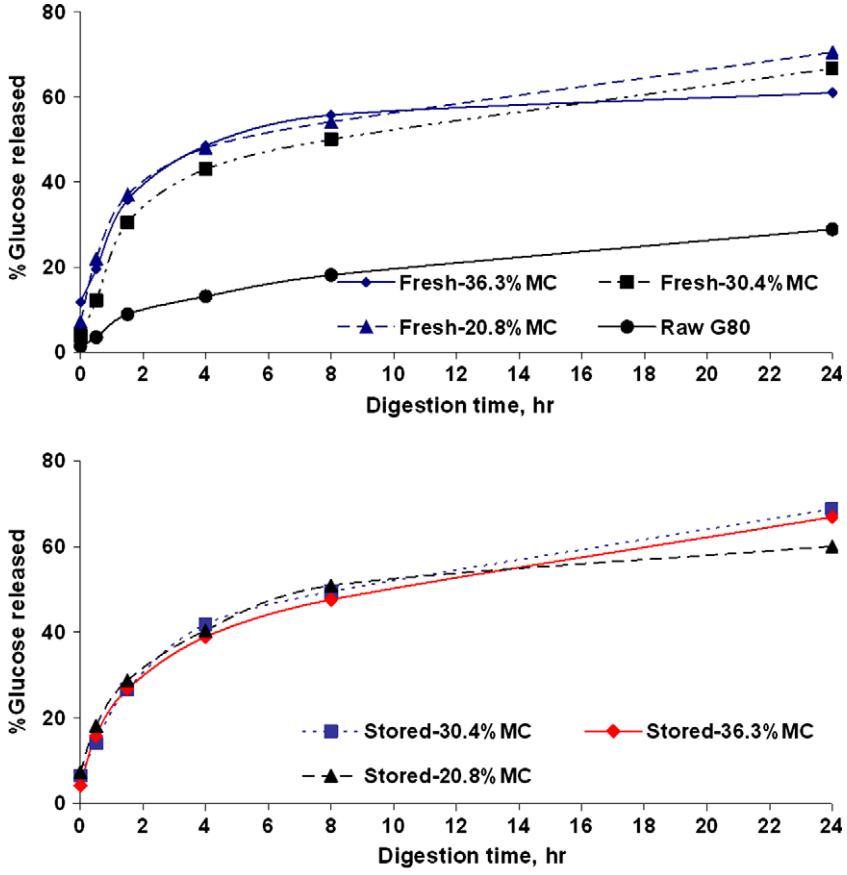

Fig. 1. Digestogram of raw, fresh and stored extruded starches after various incubation times.

Table 2
Percentage of undigested starch residues collected after digestion of raw and extruded Gelose 80 at various incubation times[a,b].

Samples	% Undigested starch residues collected at various digestion times (min)					
	0	30	90	240	480	1440
Raw Gelose 80	91.6 ± 1.6	91.4 ± 1.0	87.2 ± 21	79.0 ± 0.4	72.4 ± 0.5	57.9 ± 1.0
Extrudates						
Fresh – 20.8% MC	88.6 ± 0.6	74.2 ± 1.8	59.6 ± 1.5	48.0 ± 0.1	36.0 ± 0.9	26.4 ± 1.7
Stored – 20.8% MC	88.2 ± 0.5	69.8 ± 0.7	56.3 ± 1.9	44.5 ± 0.4	33.3 ± 0.3	28.7 ± 1.0
Fresh – 30.4% MC	91.8 ± 2.7	77.6 ± 0.1	71.2 ± 3.1	51.9 ± 1.1	39.7 ± 2.7	30.3 ± 1.5
Stored – 30.4% MC	90.3 ± 1.8	78.5 ± 0.5	66.1 ± 2.8	51.2 ± 1.3	41.3 ± 0.8	29.1 ± 0.3
Fresh – 36.3% MC	85.6 ± 2.1	79.8 ± 3.6	63.2 ± 1.1	49.8 ± 1.8	41.2 ± 0.7	32.1 ± 1.0
Stored – 36.3% MC	94.4 ± 2.3	80.3 ± 7.7	67.0 ± NA[c]	53.1 ± 9.7	40.5 ± NA	32.6 ± 0.7

[a] All data are expressed as moisture free basis.
[b] Mean ± standard deviation (of duplicates).
[c] NA means data not available.

lysis after 24 h was highest for 20.8% extrudate followed by 30.4% and 36.3%, indicating lower digestibility of Gelose 80 extruded at higher moisture content. The digestogram showed a trend of slightly declining digestibility for all stored extruded starches compared to fresh samples (Fig. 1). The effect of 12 days storage on %digestibility (ERS) of the extrudates for all three moisture contents was, however, only minor and not significant.

Residues of raw and extruded Gelose 80 samples left after the completion of digestion at each incubation time were collected. The amount of residue was calculated as %yield [(wt. of dry residue × 100)/wt. of sample], and decreased with increase in incubation time, with data complementary to and consistent with the amount of glucose released (Table 2). This gives a rough estimation of enzyme-resistant starch at each digestion time. The measurement of %yield, however, is only an estimate as complete removal of supernatant from the hydrolysate is difficult and there is always some loss of fine solids during freeze drying.

3.4. X-ray diffraction

X-ray diffraction was chosen to monitor the changes in crystal structure in the extruded starch. X-ray diffraction patterns of raw and extruded Gelose 80 and their digested residues are shown in Fig. 2. The raw Gelose 80 showed a typical B-type crystallinity with major signals at 5.5°, 17°, 22°, 23.9° and an unresolved doublet at 14° and 15° 2θ. It also shows some evidence of V-type crystallinity with a peak at 19.8° 2θ. In granular starch, the contribution from B-type crystals to the total crystallinity was 10 times higher than that of V-type crystals (cf. Table 3). The V-polymorphs have been assigned to closely packed single helices of amylose (including lipid complexes) which exist along with B-polymorphs in high amylose native starch granules (Blaszczak et al., 2005; Chanvrier et al., 2007; Shamai, Bianco-Peled, & Shimoni, 2003; Sievert, Czuchajowska, & Pomeranz, 1991).

All the extruded starches retained the signature peaks of B- and V-type polymorphs as shown by 17°, 19.8° and 22° 2θ peaks, but a certain evolution towards C-type crystallinity was observed in the samples extruded at the lowest moisture content as evidenced by a single major peak at 22–24° 2θ as opposed to two peaks (Fig. 2). However, the B-type peaks were less intense and broader compared to raw starch indicating a change in both the extent and degree of crystalline perfection in the long range molecular order of extruded starch. Past studies have shown that high amylose starches typically retain a significant level of crystallinity even after pressure cooking/extrusion whereas low amylose starches lose their granular structure associated with melting of crystallites and underlying helices, generating a more or less amorphous structure after extrusion (Blaszczak et al., 2005; Chanvrier et al., 2007). Our previous study showed that processing with a capillary rheometer lowers the short range and long range molecular order in high amylose starch e.g., a decrease of % crystallinity of raw Gelose 80 from 17.6% to 6.5% (Htoon et al., 2009) and 23% to 7.8% (Chanvrier et al., 2007).

It was evident from the current X-ray diffraction data that the changes in crystalline order in extruded starches vary with the extrusion conditions. In the extrudates, besides losing a significant portion of B-type crystallinity, there was a change in the amount of V-type crystallinity. For example, the starch extruded at the lowest moisture content (fresh sample – 20.8% moisture) had decreased B-type crystallinity from 21.1% to 11.6%, but contained more V-type crystallinity than the raw starch, e.g., 2.1% versus 3.9%, as evidenced by peaks around 7.5°, 13° and 19.8° 2θ. The intensity of

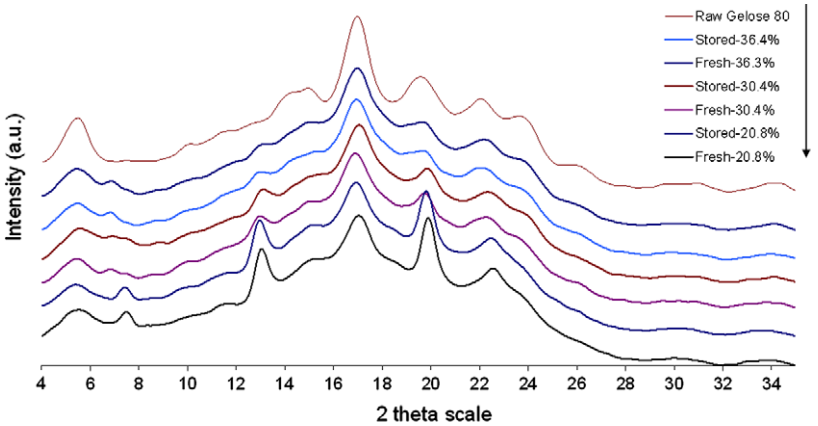

Fig. 2. Crystallinity (X-ray diffraction) analysis of the raw and extruded Gelose 80. Data have been offset for clarity.

Table 3
Changes in percentage crystallinity of raw Gelose 80 during extrusion and storage.

Samples	% Crystallinity (total, B + V)	% Crystallinity (V-type)
Raw Gelose 80	23.2	2.1
Extrudates		
Fresh – 20.8% MC	15.5	3.9
Stored – 20.8% MC	14.9	3.3
Fresh – 30.4% MC	12.1	1.8
Stored – 30.4% MC	12.5	1.9
Fresh – 36.3% MC	11.8	1.1
Stored – 36.3% MC	12.5	1.1

these V-type peaks in the lowest moisture extrudate (20.8%) was particularly marked (Fig. 2) and much more than for the highest moisture extrudate (36.6% MC) (Table 3). In fact, V-type crystallinity represents 22–25%, 11–12% and 7% of the total crystallinity from the 20.8%, 30.4% and 36.3% MC extrudates, respectively. Moreover, the positions of these peaks also vary amongst samples. See, for instance, the peak around 7° 2θ which is centred at 7.5° for the lowest moisture sample, at 7° for the highest one and two peaks are apparent in the sample extruded at 30.4% moisture. This result is probably related to the degree of hydration of the V-type crystals.

X-ray diffractograms showed that storage had only a minor effect on crystal content and morphology of the extruded starches (Table 3). The evolution of crystallinity in stored processed starch is known to differ with the source and composition of starch and the storage conditions. Bello-Perez et al. (2005) reported that extrusion of banana starch completely gelatinized the native A- and B-type crystallites. When stored, the amorphous structure of the freshly extruded banana starch slowly acquired small diffraction peaks, giving rise to the typical A-type crystalline pattern after 20 h of storage. Another study showed that after 2 days storage, the amorphous structure of freshly extruded potato starch acquired its native B-type polymorph at room temperature (22 °C) but reverted to A-type when stored at higher temperature (60 °C) (Farhat et al., 2001). Recrystallisation from high water content and/or low temperature conditions lead to the B polymorph whilst low water content and/or high temperatures yielded the A form in line with expectations (Gidley, 1987). Chanvrier et al. (2007) reported that the level of crystallinity in processed high amylose starch (Gelose 80) increased only slightly (~13% compared to control) when stored for 72 h at 4 °C but a marked increase was observed after storage at 30 °C (~44%) and 60 °C (~77%). Considering the low temperature storage of high amylose extrudates in the current study, the small increase in crystallinity is consistent with previous studies.

The digested residues from raw and extruded Gelose 80 retained both B- and V-type crystallinity (Fig. 3). Table 4 shows that V-type crystallinity at 30.4% MC contributed about 12% of the total crystallinity for both raw and extruded starches. Interestingly, the evolution of total crystallinity during digestion of raw and processed starch was different. The raw Gelose 80 had 23.2% crystal-

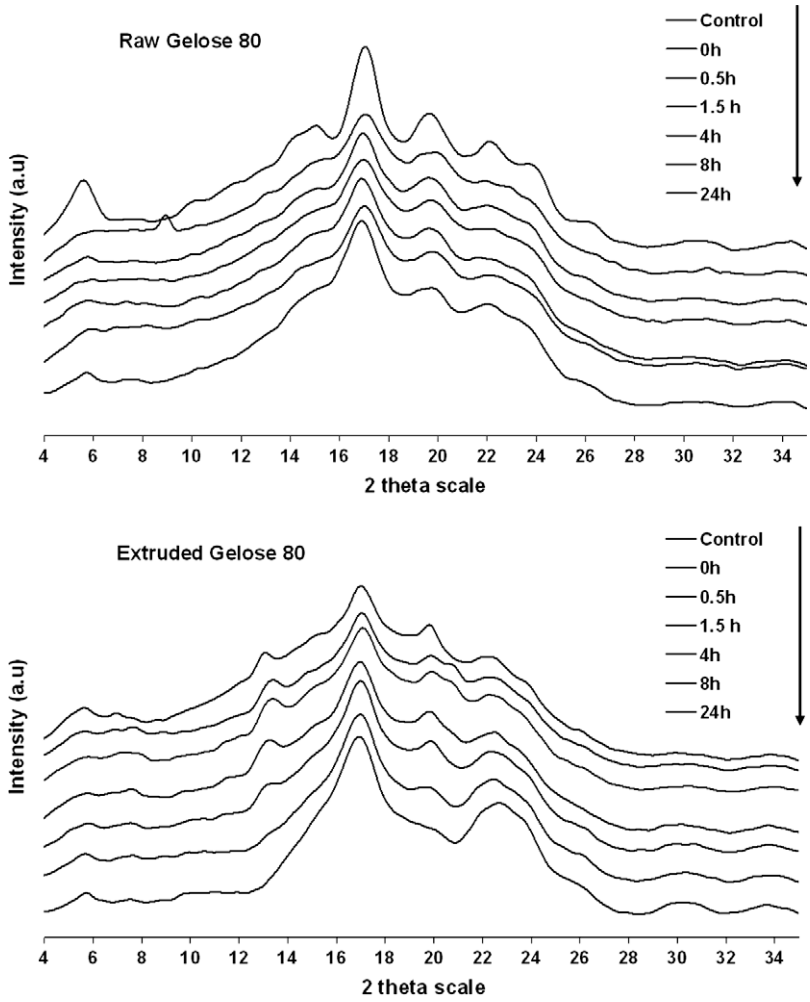

Fig. 3. Evolution of crystallinity as a function of digestion time for raw and extruded Gelose 80 (stored – 30.4% moisture). Data have been offset for clarity.

Table 4
Changes in % crystallinity of raw and extruded Gelose 80 (stored – 30.4% moisture) during incubation with starch hydrolysing enzymes.

Incubation time (h)	Raw Gelose 80		Extruded Gelose 80	
	% Crystallinity (total)	% Crystallinity (V-type)	% Crystallinity (total)	% Crystallinity (V-type)
0.0	14.2	1.6	15.4	2.1
0.5	14.0	1.3	18.4	3.0
1.5	12.6	1.2	18.7	2.7
4.0	13.0	1.1	24.3	1.4
8.0	17.6	1.2	29.5	0.4
24.0	20.7	1.4	37.7	0.2

linity which decreased to 14.2% after simulated mouth and stomach action (0 h – see Section 2). Crystallinity decreased slightly to 13% after 4 h incubation. However, the crystallinity started to increase again after 8 h incubation and reached more than 20% after 24 h (Table 4). On the other hand, the percentage crystallinity of extruded starch was 15.5% dry (Table 1) and 15.4% after simulated mouth and stomach action, and gradually increased with enzyme incubation time, finally reaching more than 37% after 24 h incubation (Table 4). The raw starch has a highly compact structure containing both crystalline and amorphous structures. For several cereal starch granules, digestion of crystalline and amorphous structures occurs side-by-side (Zhang, Ao, & Hamaker, 2006), causing no major change in overall crystallinity. High amylose maize starch granules approximately follow this trend for the early stage of digestion, but the later stages are accompanied by an increase in crystallinity of undigested residues. This could be due to either the preferential digestion of non-crystalline regions, or to active recrystallisation of partially digested polymer fragments after extended times (Htoon et al., 2009). Quantitative comparisons of yield (Table 2) versus crystallinity (Table 4) show that results could be consistent with crystalline zones being unaffected by enzyme digestion i.e. only non-crystalline regions are digested. However, for the case of granular high amylose starch in this study, some recrystallisation during the latter stages (>4 h) of digestion is suggested by the data. For instance, after 4 and 24 h, incubation yields of 79% and 58% (Table 2) and crystallinity values of 13.0% and 20.7% (Table 4) are found, respectively. If there was no recrystallisation and only non-crystalline regions were hydrolysed between 4 and 24 h, i.e. yield and crystallinity had an inverse linear relationship, the predicted 24 h crystallinity would be $(79 \times 13)/58 = 17.7\%$. As the measured value is higher, this shows that active recrystallisation occurs at least during this stage of the hydrolysis process. The fact that recrystallisation occurs in high amylose maize starch granules during enzyme digestion and not lower amylose counterparts (Zhang et al., 2006) is proposed to be due to the more rapid formation of double helices from both amylose molecules and the longer branches of amylopectin that are present to a greater extent in higher amylose maize starches.

Jane and Robyt (1984) proposed a structure for retrograded amylose in which there are crystalline, double-helical regions that are ca. 10 nm long, interspersed with amorphous regions. The amorphous regions are considered to be hydrolysed by acids/α-amylase leaving the crystalline regions intact. Our current findings are not fully consistent with this model, as the crystallinity of undigested residues after 24 h enzyme treatment is no more than 38% i.e. there is always a majority of non-crystalline material. It is clear from this and a previous study (Htoon et al., 2009) that non-crystalline amylose-rich starches can exhibit long-term enzyme resistance.

3.5. FTIR spectroscopy

Infrared spectroscopy in the spectral region of 800–1200 cm^{-1} was used to further investigate the changes in starch structure of raw and extruded Gelose 80 and their enzyme-indigestible residues. The IR spectrum of all extruded starches appeared to be the same as all peaks were at the same position and had almost the same intensity, differing only from raw starch (Fig. 4). All the peaks at 1045 and 995 cm^{-1} for extruded starch were slightly lower than for raw starch but higher at 1022 cm^{-1}. Various studies have shown that the band intensities at these three wave numbers are sensitive to changes in starch conformation as inferred from X-ray diffraction (Goodfellow & Wilson, 1990; van Soest, Tournois, de Wit, & Vliegenthart, 1995) or differential scanning calorimetry (Bello-Perez et al., 2005). The band at 1022 cm^{-1} has been correlated with the vibrational modes within the amorphous phase of starch as this band has been observed to decrease with increasing crystallinity (Lopez-Rubio, Flanagan, Shrestha et al., 2008; Rubens & Heremans, 2000). The bands at 1045 or 1047 and 995 cm^{-1} have been linked with a high degree of order/crystallinity in starch molecules (Sevenou, Hill, Farhat, & Mitchell, 2002; van Soest et al., 1995). The intensity ratio of 1045/1022 or 995/1022 cm^{-1} has been used as a convenient index for estimating the degree of molecular order in starch molecules (Bello-Perez et al., 2005; Lopez-Rubio, Flanagan, Shrestha et al., 2008; van Soest et al., 1995).

Fig. 5 shows that extrusion of raw Gelose 80 caused a significant reduction in the 995/1022 cm^{-1} ratio indicating a change in short range molecular order, consistent with the X-ray diffraction finding that extrusion reduces crystallinity. The 995/1022 cm^{-1} ratio, however, did not systematically vary with feed moisture or storage time, despite the differences in crystalline polymorph detected by X-ray diffraction (Fig. 2). There was no difference in 995/1022 cm^{-1} ratio with increasing moisture content and only minor changes were observed due to storage (Fig. 5). In a similar study, Bello-Perez et al. (2005) reported a sharp increase in the peak intensities of 995 and 1045 cm^{-1} and decrease in 1022 cm^{-1} for raw banana at 0.5 h after extrusion and after 24 h storage. This change was assigned to the retrogradation of banana starch (as supported by DSC, X-ray diffraction and ERS results). In the case of our samples, a lack of difference in X-ray diffraction and digestibility between fresh and stored extrudates across the moisture contents (Tables 1–3) is consistent with the similarity in FTIR spectra.

Fig. 5 also shows the IR spectra of both raw and extruded starches enzyme digested from 0 to 24 h. FTIR spectra of raw starch and the resultant residues at different times of digestion did not vary significantly and no noticeable change in intensity of signature peaks was noticed. The comparison of intensity ratio 995/1022 cm^{-1}, however, suggested an initial decrease in short range order of raw starch molecules followed by final increase after 24 h of incubation, consistent with X-ray diffraction data (Table 4). In digested extruded starches, the IR spectra clearly showed that, with the progression of incubation times, the peaks around 1045 and 995 cm^{-1} become steeper whereas the peak around 1022 cm^{-1} was flatter. This observation is also supported by a gradual increase in the 995/1022 cm^{-1} ratio with incubation time (Fig. 5). These results are in qualitative agreement with data from X-ray diffraction and resistant starch analysis, showing a general trend of increased crystallinity in long time digestion residues

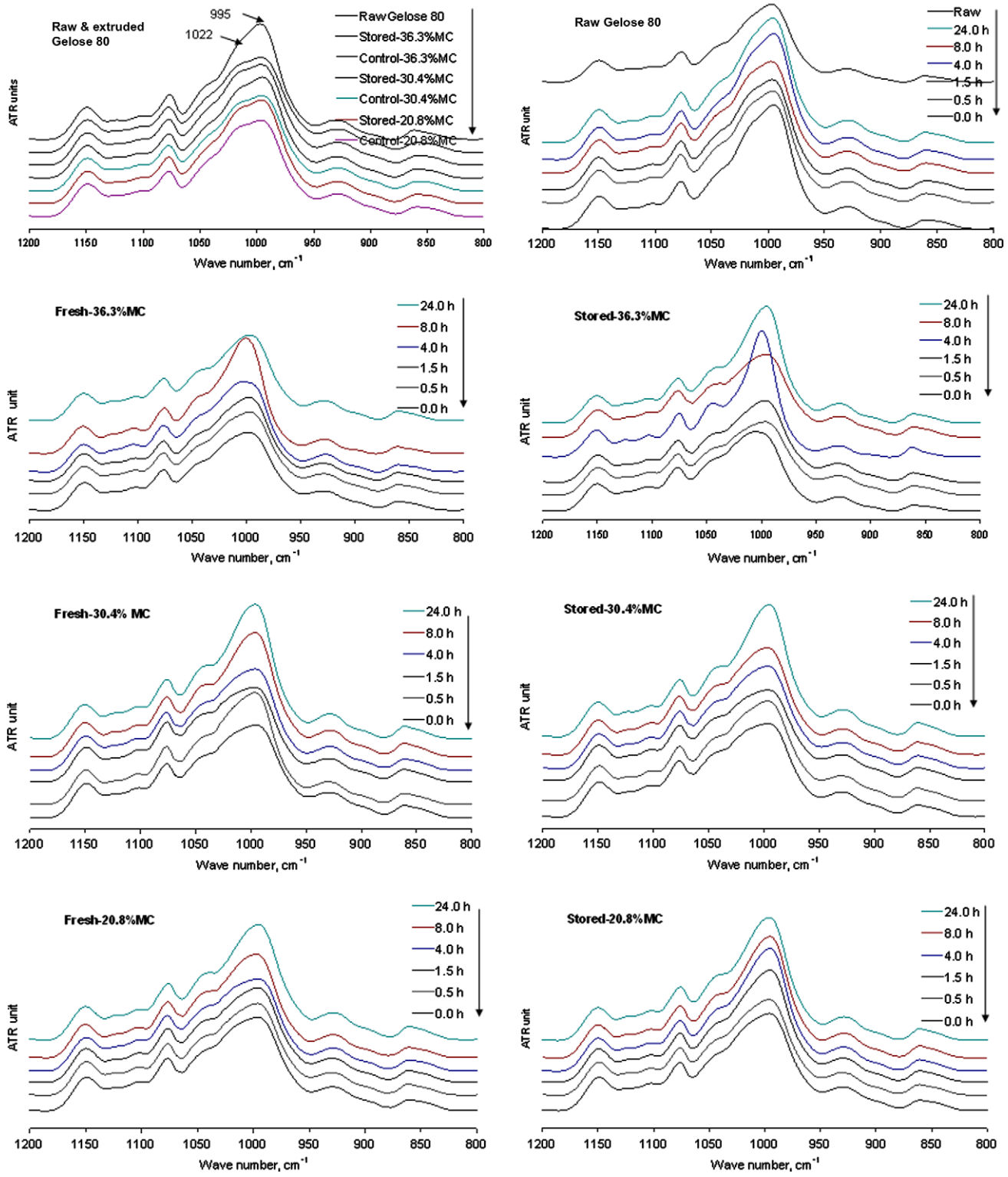

Fig. 4. FTIR spectra in Gelose 80 extruded at various extrusion conditions and evolution of FTIR spectra during digestion of raw and extruded Gelose 80 from 0 to 24 h. Data have been offset for clarity.

when compared with the more amorphous nature of extruded starches.

3.6. Microscopy

The morphology of raw and extruded starches together with digestion-resistant residues was analysed by optical and scanning electron microscopy. The SEM image of raw Gelose 80 showed apparent unimodal size distribution and irregular shape (Fig. 6B) as reported previously by others (Jane, Kasemsuwan, Leas, Zobel, & Robyt, 1994). Polarized light microscopy showed a characteristic birefringence pattern with a Maltese cross centred at the hilum (Fig. 6A). The Maltese cross for high amylose starch was distorted compared to lower amylose maize starches, presumably because of

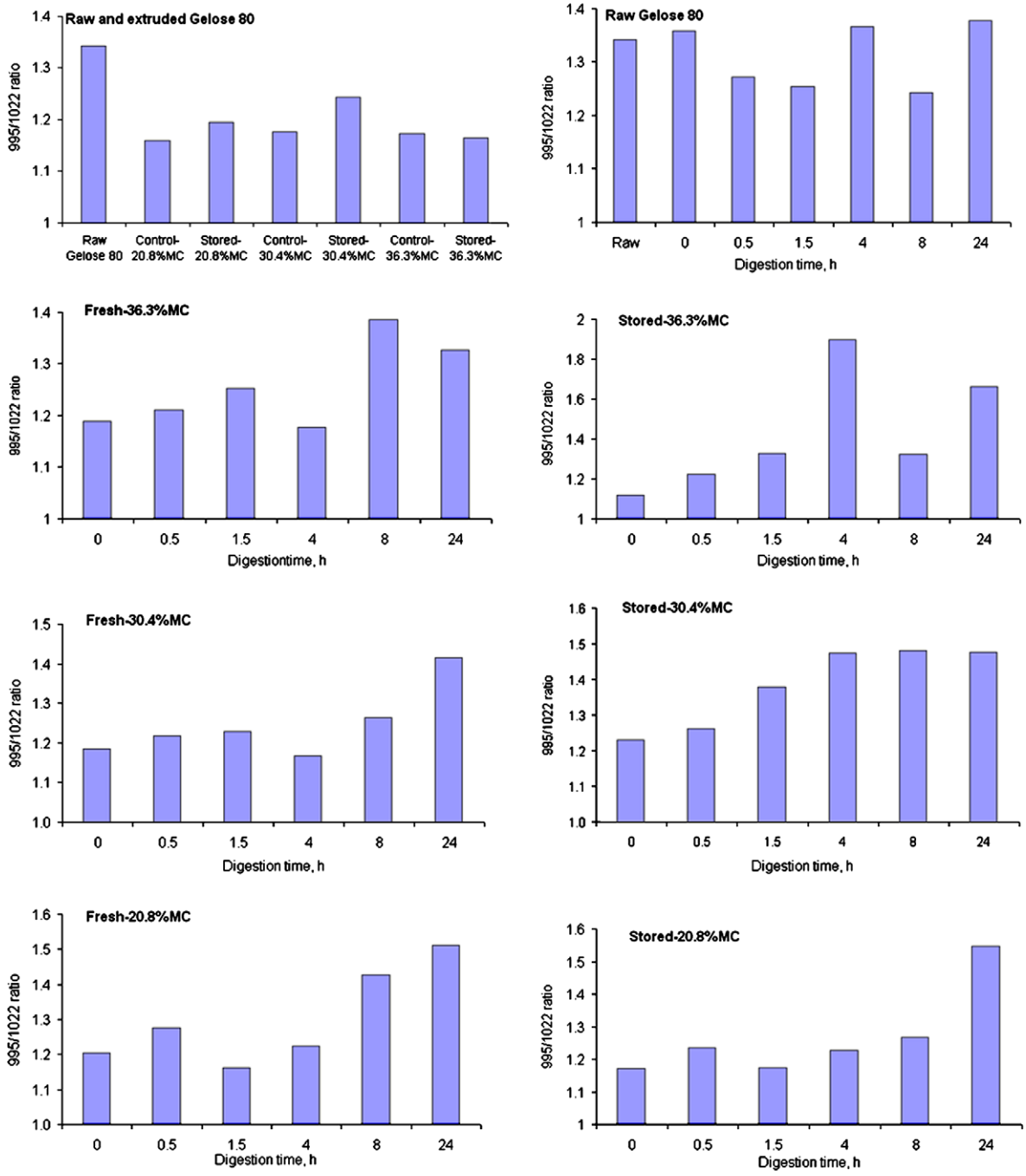

Fig. 5. Ratio of FTIR spectra at 995/1022 in Gelose 80 extruded at various extrusion conditions and changes in 995/1022 ratios during digestion of raw and extruded Gelose 80 from 0 to 24 h.

the low level of ordered amylopectin within the lamellar structure responsible for the birefringence pattern. Extrusion and cryo-milling appeared to result in both fragmentation and aggregation of starch granules, resulting in aggregates of varying size, shape, and thickness (Fig. 6G). Previous SEM images of oven dried and hammer milled (or mortar and pestle ground) processed HAMS also showed aggregates and a significant number of fragments (Lopez-Rubio, Flanagan, Shrestha et al., 2008). When viewed under polarized light, strong birefringence was observed in the aggregates but without apparent Maltese crosses (Fig. 6F). This is consistent with the presence of measurable crystallinity (Fig. 2) leading to birefringence, but loss of the regular radial arrangement of lamellar structures within granules resulting in the absence of a Maltese cross pattern.

Incubation of starch granules for 1.5 h with hydrolysing enzymes (Fig. 6C) roughened the originally smooth granule surface due to multiple enzyme attack (~9% starch digested). There was heterogeneity in starch granule degradation (Fig. 6C and D) as some granules were extensively hydrolysed by enzymes whereas others were hardly attacked. The localized attack by enzymes also resulted in small pits on the surface of a few granules ('exo corrosion', see inset in Fig. 6C). With the progression of digestion, the roughened surface enlarged into large 'fissures', described as a 'saw tooth pattern' by Planchot et al. (1995). In some granules, enzyme attack on the pits continues, forming large holes deeper into the granules through 'endo corrosion' (Fig. 6D). Similar patterns of attack continue on the granules resulting in multiple holes and some granules almost collapsing due to hydrolysis from the inside

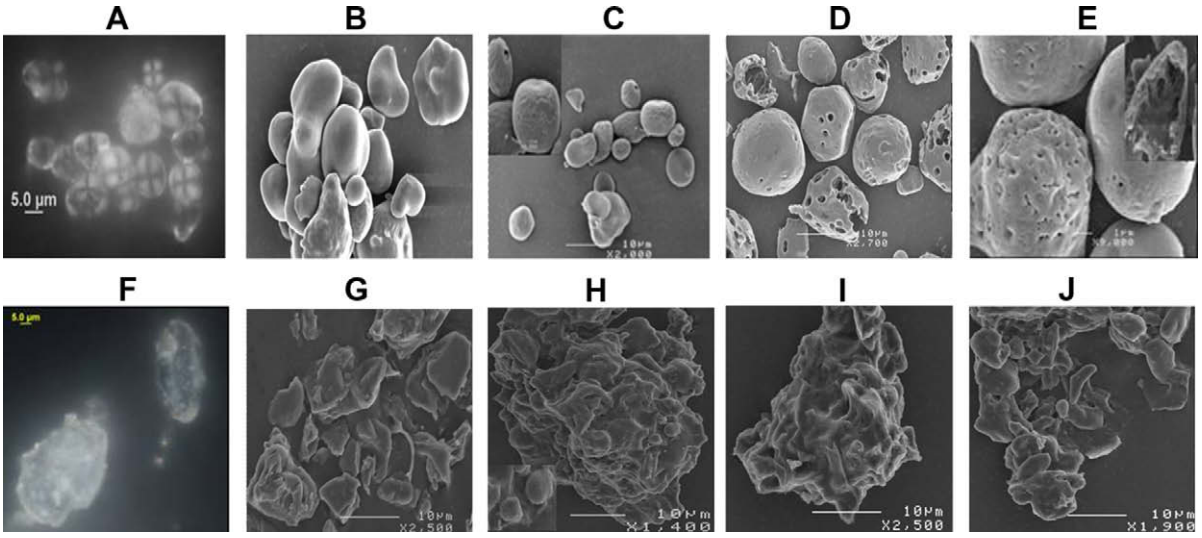

Fig. 6. Polarized light microscopy and SEM images of raw and extruded Gelose 80 (stored 30.4% water) and residues after different digestion times. Upper row: (A) raw starch under polarized light; (B)–(E) SEM images of raw and digested raw starch after 1.5, 4 and 24 h incubation, respectively. Lower row: (F) extruded starch under polarized light; (G)–(J) SEM images of extruded and digested extruded (stored – 30.4% water) starch after 1.5, 4 and 24 h incubation, respectively.

towards the periphery (see inset, Fig. 6E). Considering that about 50% of Gelose 80 had been digested after 24 h incubation (Fig. 1), it was not surprising to see a significant number of partially digested starch granules by SEM.

Unlike raw starch, the pattern of enzyme hydrolysis on extruded starch is less clear as all the granules are heavily damaged and fused to one another, although the outline of individual granules is still obvious. The initial mode of enzyme digestion, e.g., after 0.5 h, involved attack on the surface of starch aggregates as shown by holes of different size on the surface of extruded starch (Fig. 6H, residue after 22% digested). Interestingly, some small intact granules were observed on the surface of the aggregate (magnified picture shown as inset in Fig. 6H). This shows that not all granules are destroyed during extrusion cooking and some remain apparently intact, 'hidden' within the sheared starchy mass. With the progression of digestion, after 4.0 h the starch aggregates appear more smooth and fused due to enzyme attack (Fig. 6I, residue after 48% digested). No starch granules were visible on the surface of aggregates. At later stages of incubation, >24 h, the aggregates are smaller in size showing the progression of the digestion process (Fig. 6J).

3.7. Conclusions

High amylose maize starch has been shown to be a robust and potentially useful nutritional source of enzyme-resistant starch, even after high temperature extrusion processing. Whilst the granular form offers exceptional levels of ERS (>50%), this form is not usually compatible with palatable food formulations. The fact that HAMS still contains 10–20% ERS after a range of simple extrusion processing conditions offers the possibility of formulating foods to realistically achieve high levels of enzyme-resistant starch intake.

Whilst extrusion processing of HAMS results in obvious macroscopic modification (Fig. 6), the resultant products still have significant crystalline order. By comparing the percentage of undigested residues with their corresponding amount of crystallinity at different times of digestion for granular Gelose 80, it would appear that recrystallisation during digestion is, at least partly, responsible for the resulting crystalline order. For extruded starches, undigested residues have increasing crystallinity during digestion consistent with either exclusive hydrolysis of non-crystalline regions, or recrystallisation during digestion. Irrespective of the initial crystallinity, moisture content or storage of the extrudates, enzyme digestion rates were all very similar. Together with the relatively low levels of crystallinity in undigested fractions, this suggests that enzyme resistance is associated with a dense solid phase structure that is only weakly-crystalline, and that measures of crystallinity are not sufficient to predict enzyme resistance. Further work is needed to better characterise this largely amorphous material to understand the structural origins of enzyme resistance.

References

Agustiniano-Osornio, J. C., Gonzalez-Soto, R. A., Flores-Huicochea, E., Manrique-Quevedo, N., Sanchez-Hernandez, L., & Bello-Perez, L. A. (2005). Resistant starch production from mango starch using a single-screw extruder. *Journal of the Science of Food and Agriculture, 85*, 2105–2110.

Al-Rabadi, G. J. S., Gilbert, R. G., & Gidley, M. J. (2009). Effect of particle size on kinetics of starch digestion in milled barley and sorghum grains by porcine alpha-amylase. *Journal of Cereal Science, 50*, 198–204.

Annison, G., & Topping, D. (1994). Nutritional role of resistant starch: Chemical structure vs physiological function. *Annual Review of Nutrition, 14*, 297–320.

Asp, N.-G. (1992). Resistant starch. *European Journal of Clinical Nutrition, 46*(Suppl. 2), S1.

Bello-Perez, L. A., Ottenhof, M. A., Agama-Acevedo, E., & Farhat, I. A. (2005). Effect of storage time on the retrogradation of banana starch extrudate. *Journal of Agriculture and Food Chemistry, 53*, 1081–1086.

Berry, C. S. (1986). Resistant starch: Formation and measurement of starch that survives exhaustive digestion with amylo-lytic enzymes during the determination of dietary fibre. *Journal of Cereal Science, 4*, 301–314.

Bird, A. R., Lopez-Rubio, A., Shrestha, A. K., & Gidley, M. J. (2009). Resistant starch in vitro and in vivo: Factors determining yield, structure, and physiological relevance. In S. Kasapis, I. T. Norton, & J. B. Ubbink (Eds.), *Modern biopolymer sciences* (pp. 449–512). London: Academic Press.

Blaszczak, W., Fornal, J., Valverde, S., & Garrido, L. (2005). Pressure-induced changes in the structure of corn starches with different amylose content. *Carbohydrate Polymers, 61*, 132–140.

Cairns, P., Botham, R. L., Morris, V. J., & Ring, S. G. (1996). Physiochemical studies on resistant starch in vitro and in vivo. *Journal of Cereal Science, 23*, 265–275.

Cairns, P., Sun, L., Morris, V. J., & Ring, S. G. (1995). Physicochemical studies using amylose as an in-vitro model for resistant starch. *Journal of Cereal Science, 21*, 37–47.

Champ, M. (2004). Resistant starch. In A. Eliasson (Ed.), *Starch in food structure, function and applications* (pp. 560–574). England, Cambridge: Woodhead Publishing Limited.

Chanvrier, H., Uthayakumaran, S., Appelqvist, I. A. M., Gidley, M. J., Gilbert, E. P., & López-Rubio, A. (2007). Influence of storage conditions on the structure, thermal behavior, and formation of enzyme-resistant starch in extruded starches. *Journal of Agriculture and Food Chemistry, 55*, 9883–9890.

Eerlingen, R. C., Bjorck, I. V. D., Delcour, J. A., Slade, L., & Levine, H. (1994). Enzyme-resistant starch. VI. Influence of sugars on resistant starch formation. *Cereal Chemistry, 71*, 472–476.

Eerlingen, R. C., Cillen, G., & Delcour, J. A. (1994). Enzyme-resistant starch. IV. Effect of endogenous lipid and added sodium dodecyl sulfate on formation of resistant starch. *Cereal Chemistry, 71*, 170–177.

Eerlingen, R. C., Crombez, M., & Delcour, J. A. (1993). Enzyme resistant starch. I. Quantitative and qualitative influence of incubation time and temperature of autoclaved starch on resistant starch formation. *Cereal Chemistry, 70*, 339–344.

Englyst, H. N., Kingman, S. M., & Cummings, J. H. (1992). Classification and measurement of nutritionally important starch fractions. *European Journal of Clinical Nutrition, 46*, 33–50.

Escarpa, A., Gonzalez, M. C., Morales, M. D., & Saura-Calixto, F. (1997). An approach to the influence of nutrients and other food constituents on resistant starch formation. *Food Chemistry, 60*, 527–532.

Evans, A., & Thompson, D. B. (2004). Resistance to alpha-amylase digestion in four native high-amylose maize starches. *Cereal Chemistry, 81*, 31–37.

Farhat, I. A., Protzmann, J., Becker, A., Valles-Pamies, B., Neale, R., & Hill, S. E. (2001). Effect of the extent of conversion and retrogradation on the digestibility of potato starch. *Starch/Starke, 53*, 431–436.

Ferrero, C., Martino, M. N., & Zaritzky, N. E. (1993). Stability of frozen starch pastes: Effect of freezing, storage and xanthan gum addition. *Journal Food Processing and Preservation, 17*, 191–211.

Garcia-Alonso, A., & Goni, I. (2000). Effect of processing on potato starch: In vitro availability. *Starch/Starke, 2–3*, 81–84.

Gidley, M. J. (1987). Factors affecting the crystalline type (A–C) of native starches and model compounds: A rationalisation of observed effects in terms of polymorphic structure. *Carbohydrate Research, 161*, 301–304.

Gidley, M. J., Cooke, D., Darke, A. H., Hoffmann, R. A., Russell, A. L., & Greenwell, P. (1995). Molecular order and structure in enzyme-resistant retrograded starch. *Carbohydrate Polymers, 28*, 23–31.

Goni, I., Garcia-Diz, L., Manas, E., & Saura-Calixto, F. (1996). Analysis of resistant starch: A method for foods and food products. *Food Chemistry, 56*, 445–449.

Gonzalez-Soto, R. A., Escobedo, R., Hernandez-Sanchez, H., Sanchez-Rivera, M., & Bello-Perez, L. A. (2006). The influence of time and storage temperature on resistant starch formation from autoclaved debranched banana starch. *Food Research International, 40*, 304–310.

Goodfellow, R., & Wilson, B. J. (1990). Fourier transform IR study of the gelation of amylose and amylopectin. *Biopolymers, 30*, 1183–1189.

Htoon, A., Shrestha, A. K., Flanagan, B. M., Lopez-Rubio, A., Bird, A. R., Gilbert, E. P., et al. (2009). Effects of processing high amylose maize starches under controlled conditions on structural organization and amylase digestibility. *Carbohydrate Polymers, 75*, 236–245.

Jane, J. L., Kasemsuwan, T., Leas, S., Zobel, H., & Robyt, J. F. (1994). Anthology of starch granule morphology by scanning electron microscopy. *Starch/Starke, 46*, 121–129.

Jane, J. L., & Robyt, J. F. (1984). Structure studies of amylose-V complexes and retrograded amylose by action of alpha amylases, and a new method for preparing amylodextrins. *Carbohydrate Research, 132*, 105–118.

Jenkins, P. J., & Donald, A. M. (1996). Application of small angle neutron scattering to the study of the structure of starch granules. *Polymer, 37*, 5559–5568.

Jiang, G. S., & Liu, Q. (2002). Characterization of residues from partially hydrolyzed potato and high amylose corn starches by pancreatic alpha-amylase. *Starch/Starke, 54*, 527–533.

Kendall, C. W. C., Emam, A., Augustin, L. S. A., & Jenkins, D. J. A. (2004). Resistant starches and health. *Journal of AOAC International, 87*, 769–774.

Kim, J. H., Tanhehco, E. J., & Ng, P. K. W. (2006). Effect of extrusion conditions on resistant starch formation from pastry wheat flour. *Food Chemistry, 99*, 718–723.

Liljeberg, H., Akerberg, A., & Bjorck, I. (1996). Resistant starch formation in bread as influenced by choice of ingredients or baking conditions. *Food Chemistry, 56*, 389–394.

Lopez-Rubio, A., Flanagan, B. M., Gilbert, E. P., & Gidley, M. J. (2008). A novel approach for calculating starch crystallinity and its correlation with double helix content: A combined XRD and NMR study. *Biopolymers, 89*, 761–768.

Lopez-Rubio, A., Flanagan, B. M., Shrestha, A. K., Gidley, M. J., & Gilbert, E. P. (2008). Molecular rearrangement of starch during in-vitro digestion: Towards a better understanding of enzyme resistant starch formation. *Biomacromolecules, 9*, 1951–1958.

Morita, T., Ito, Y., Brown, I. L., Ando, R., & Kiriyama, S. (2007). In vitro and in vivo digestibility of native maize starch granules varying in amylose contents. *Journal of AOAC International, 90*, 1628–1634.

Oates, C. G. (1997). Towards an understanding of starch granule structure and hydrolysis. *Trends in Food Science & Technology, 8*, 375–382.

Onyango, C., Bley, T., Jacob, A., Henle, T., & Rohm, H. (2006). Influence of incubation temperature and time on resistant starch type III formation from autoclaved and acid-hydrolyzed cassava starch. *Carbohydrate Polymers, 66*, 494–499.

Planchot, V., Colonna, P., Gallant, D. J., & Bouchet, B. (1995). Extensive degradation of native starch granules by alpha-amylase from *Aspergillus-fumigatus*. *Journal of Cereal Science, 21*, 163–171.

Ring, S. G., Gee, J. M., Whittam, M., Orford, P., & Johnson, I. T. (1988). Resistant Starch: Its chemical form in foodstuffs and effect on digestibility in vitro. *Food Chemistry, 28*, 97–109.

Rubens, P., & Heremans, K. (2000). Pressure–temperature gelatinization phase diagram of starch: An *in situ* fourier transform infrared study. *Biopolymers, 54*, 524–530.

Sevenou, O., Hill, S. E., Farhat, I. A., & Mitchell, J. R. (2002). Organization of the external region of the starch granule as determined by infrared spectroscopy. *International Journal of Biological Macromolecules, 31*(1–3), 79–85.

Shamai, K., Bianco-Peled, H., & Shimoni, E. (2003). Polymorphism of resistant starch type III. *Carbohydrate Polymers, 54*, 363–369.

Sievert, D., Czuchajowska, Z., & Pomeranz, Y. (1991). Enzyme-resistant starch. III. X-ray diffraction of autoclaved amylomaize VII starch and enzyme-resistant starch residues. *Cereal Chemistry, 68*, 86–91.

Sievert, D., & Pomeranz, Y. (1989). Enzyme-resistant resistant. I. Characterization and evaluation of enzymatic, thermoanalytical and microscopic methods. *Cereal Chemistry, 66*, 342–347.

Sievert, D., & Pomeranz, Y. (1990). Enzyme-resistant starch. 2. Differential scanning calorimetry studies on heat-treated starches and enzyme-resistant starch residues. *Cereal Chemistry, 67*, 217–221.

Szczodrak, J., & Pomeranz, Y. (1991). Starch and enzyme-resistant starch from high-amylose starch. *Cereal Chemistry, 68*, 589–596.

Themeier, H., Hollman, J., Neese, U., & Lindhauer, M. G. (2005). Structural and morphological factors influencing the quantification of resistant starch II in starches of different botanical origin. *Carbohydrate Polymers, 61*, 72–79.

Thuwall, M., Boldizar, A., & Rigdahl, M. (2006). Extrusion processing of high amylose potato starch materials. *Carbohydrate Polymers, 65*, 441–446.

Topping, D. L., & Clifton, P. (2001). Short chain fatty acids and human colonic function – Roles of resistant starch and non starch polysaccharides. *Physiological Reviews, 81*, 1031–1064.

Unlu, E., & Faller, J. F. (1998). Formation of resistant starch by a twin-screw extruder. *Cereal Chemistry, 37*, 346–350.

van Soest, J. J. G., Tournois, H., de Wit, D., & Vliegenthart, J. F. G. (1995). Short-range structure in partially crystalline potato starch determined with attenuated total reflectance Fourier-transform IR spectroscopy. *Carbohydrate Research, 279*, 201–214.

Vasanthan, T., & Bhatty, R. S. (1998). Enhancement of resistant starch (RS3) in amylomaize, barley, field pea and lentil starches. *Starke/Starch, 50*, 286–289.

Vasanthan, T., Gaosong, J., Yeung, J., & Li, J. (2002). Dietary fiber profile of barley flour as affected by extrusion cooking. *Food Chemistry, 77*, 35–40.

Zhang, G., Ao, Z., & Hamaker, B. R. (2006). Slow digestion property of native cereal starches. *Biomacromolecules, 7*, 3252–3258.